Manufacturing of precision optical coatings

Markus K. Tilsch*, Marius Grigonis, and Georg J. Ockenfuss

JDSU, Santa Rosa, CA 95407, USA

**E-mail: Markus.Tilsch@jdsu.com*

Received October 29, 2009

Thin film optical coatings tailor light reflected or transmitted from an optical element in a desired way. An optical coating chamber is a complex system in which multiple subsystems operate together to fabricate such coatings. For physical vapor deposition processes, such as evaporation and sputtering, the active parts of the subsystems are located within a vacuum chamber. One example is the source system that provides vapor from which films are formed. A gas delivery subsystem may add process gases either in their ground or excited states. Rotary motion and masking subsystems may be used to achieve better uniformity. In addition, a subsystem that ensures accurate layer thickness control may be utilized. Precision optical coatings require that individual layer thicknesses be controlled to within a few percent of the design target or less to achieve accurate placement of a spectral feature. Systems for manufacturing precision optical coatings demand the use of the subsystems that operate within tight tolerances. In this letter, we illustrate subsystem requirements by examining three examples in detail. We then discuss spectral placement impact resulting from height variations of the substrate mounting, thermal gradients on a substrate, and process instabilities from a moving anode. Finally, we conclude by providing a few examples of the performance attainable using a precision coating platform, when all subsystems work properly.

OCIS codes: 310.0310, 310.1620, 310.6845, 350.2460.

doi: 10.3788/COL201008S1.0038.

Manufacturing of precision optical coatings requires well-controlled processes for design, pre-coating, coating, and post-coating operations. In this letter, we focus on precision aspects of the coating operation.

For our discussion, we define precision coating as a coating requiring great attention to detail to meet optical requirements. The applicability level of precision depends on the size of the optic to be coated. With advancement in technology and use of sophisticated equipment in the industry, precision has substantially improved over time. To quantify precision, we express a spectral tolerance as a wavelength placement tolerance of a spectral feature divided by the nominal wavelength of that feature, expressed as a percentage. At present, spectral tolerance for coatings on relatively large optics (∼0.5 meter) is often required to be ±1% or less, while smaller optics (∼0.2 meter) is often required to be ±0.4% or less. Filters for telecommunication applications are often only a millimeter or two in size, but spectral tolerance must be controlled to less than ±0.01%, and sometimes even less than ±0.001%. Other spectral requirements like transmission levels or phase relations also drive the need for tightly precise coating controls.

In a coating process, multiple subsystems work together. A technology to provide coating vapor is utilized. Modern physical vapor deposition techniques, which include sputtering and evaporation, are often augmented with energetic ions to yield stable, dense, and high-quality optical films. A reactive gas may be delivered. One or more methods may be added to control the process, such as stabilizing a sputter process at a specific hysteresis value or controlling deposition rate of an evaporative system. Substrates are typically put into motion (e.g., rotary motion) to increase coating uniformity across them. In addition, stationary or moving masks may be utilized to further improve uniformity. A thickness monitoring method may be used to control the thickness of layers. All these process subsystems must operate together to ensure that the precision coating is properly manufactured. On the contrary, for any of these subsystems, operating outside tolerance levels could prohibit the success of the coating batch.

In this letter, we discuss three examples that demonstrate how requirements for a precision coating could drive the requirements for the mechanical system, the thermal system, and the design for process components. When all of the process subsystems of a well-designed coating chamber operate within their specifications, impressive results can be achieved. We conclude by providing several examples of the performance obtained using the JDSU Ucp-1 coating platform[1,2].

Coating equipment often employs a complex rotary motion system to minimize coating non-uniformity across parts of the system. Mechanical precision is an important aspect for producing optical coatings with tightly controlled spectral placement. A rotary motion system consists of a large number of mechanical components that are assembled together. The stack-up of tolerances of these components impacts the location of substrates, therefore affecting coating geometry and spectral performance of coated products.

We considered the example of a planetary rotation system, such as one implemented in JDSU's Ucp-1 platform[1,2]. The schematic of the Ucp-1 planetary rotation system is presented in Fig. 1. Substrates are attached to the planets, and planets are mounted to spindles held on the carrier plate, allowing each planet to rotate around its axis. The carrier plate is affixed to the main rotary motion shaft that is coupled to a motor shaft. As the motor rotates the carrier plate, a certain amount of its rotational momentum is transferred to the planets. This is typically accomplished with the help of a system of gears. The resulting action is a double rotation: a rotating carrier plate and individually rotating planets. In the case of Ucp-1, the drive consists of six rotating planets to which substrates for deposition (200-mm diameter)

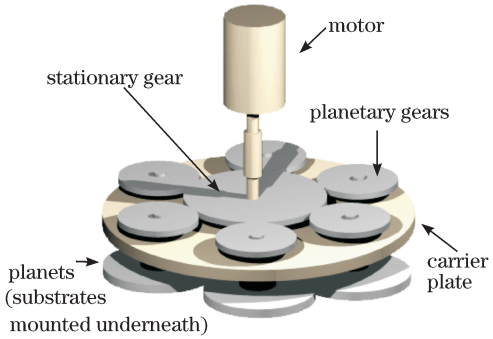

Fig. 1. Schematic of a planetary rotary drive system.

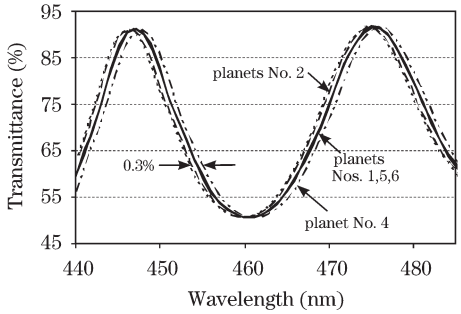

Fig. 2. Spectral measurements of a coating deposited on 6 planets.

are attached. The sputter coating source (not shown in Fig. 1) is positioned underneath the rotary drive system.

Each planet constitutes a relatively complex, but nevertheless independent system, of a large number of components, such as shafts, bearings, gears, and couplings. Tolerance stack-up will likely differ for each planet, thus causing significant difference in terms of vertical positioning of the coating surface of each planet relative to the carrier plate. Carrier plate flatness and mounting perpendicularity to the main rotary motion shaft also affects vertical positioning of the planets. Similarly, inadequate manufacturing tolerances for the main shaft or the supporting bearing system may result in non-perpendicularity of the carrier plate relative to the main rotation axis. For example, for a 750-mm diameter carrier plate, a non-perpendicularity of 0.2 degree results in ±1.3-mm vertical displacement at the outer edge of the carrier plate. All abovementioned contributions determine the absolute vertical position of the coating surface of each planet. The distance between the coating surface and the coating source influences the coating rate, and thus, spectral placement.

A good way to assess planet-to-planet spectral performance is to deposit a coating structure with one or more well-defined spectral features. Variation in spectral placement from planet to planet is a good measure of how well a rotary drive system is optimized.

Figure 2 shows the spectral measurements of a coating design deposited on six planets in the same run. The spread in wavelength placement of the spectral features is evident. At first glance, such "random" distribution is difficult to explain. However, detailed mechanical characterization of the rotary drive system reveals that this data correlates well with vertical height distributions of the planets.

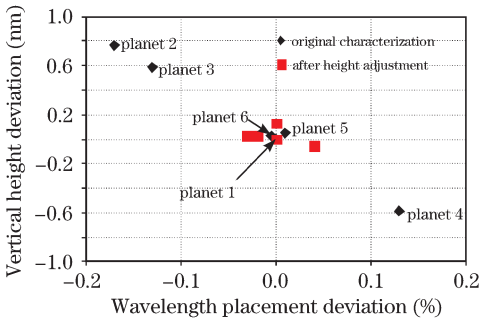

Fig. 3. Spectral placement and planet height.

Figure 3 shows the vertical height deviation of each planet versus deviation in wavelength placement of the respective filter. The black diamonds summarize the run performance from Fig. 2. The data were normalized to the vertical height and placement of planet No. 1.

The shortest wavelength is observed for planets No. 2 and No. 3, the two farthest from the coating source. In contrast, the longest wavelength is observed for planet No. 4, the planet closest to the coating source. The spectral placement for planets Nos. 1, 5, and 6 is very similar, which is also the case for the vertical positioning of these planets.

The placement variation on vertical height variation depends largely on a specific coating geometry. For the Ucp-1 platform, a change of 1 mm in vertical distance results in a change of spectral placement by 0.22%.

The red squares in Fig. 3 show the resulting performance after adjusting the vertical heights of the six planets to minimize height variation. All planet heights were set within a 0.2 mm range. The spread in wavelength placement of the planets was significantly reduced, and in this particular case, turned out to be within 0.1%. To produce coatings with precise spectral placement, a tight vertical positioning control is very important.

Wavelength division multiplexing telecommunications filters have extremely tight tolerances[3]. Typically, coating is applied on a disk-shaped substrate (100 to 300 mm in diameter), which is diced and thinned during the post-deposition steps. During deposition, the substrate is spun at a high rotational frequency in a single rotation to ensure good uniformity. Channel spacing for 100 GHz bandpass filters is only about 0.8 nm at 1550 nm. This correlates to a difference of 0.05% in layer thicknesses of filters from adjacent channels. For a predictable process, it is desirable to control coating thickness distribution across the targeted good area of the substrate to that precision level or better.

Non-uniformity in a single rotation system can be described by a radial and azimuthal component. We define radial non-uniformity as the variation in coating thickness from center to the outside part of disk. Radial non-uniformity must be minimized through optimization of coating geometry, and in some cases, through the application of proper masking. Azimuthal non-uniformity is the change in coating thickness around the disk when measured at a fixed radius. In an ideal, absolutely symmetrical, high-speed single rotation system, we expect no azimuthal non-uniformity. However, this may not the case in actual setting. As discussed in the previous

examples, the distance of substrate to the coating source needs to be tightly controlled. If the substrate coating surface plane is not maintained exactly perpendicular to the rotation center axis, one side of the substrate will be systematically located further away from the coating source than the other side. For the 100 GHz filter, mechanical tolerances of less than 0.1 mm may be required.

At JDSU, we initially employed a substrate-mounting hub with a large, plane contact surface between substrate and hub. Maintaining a plane surface over multiple runs proved to be difficult. To make the mounting hub more deterministic, we fabricated a three-point contact hub, as shown in the top-down view sketch in Fig. 4. In this hub, three precision contact points touched the back of the substrate at radius R_1. The precision contacts were adjusted in height, thus allowing optimization of contact

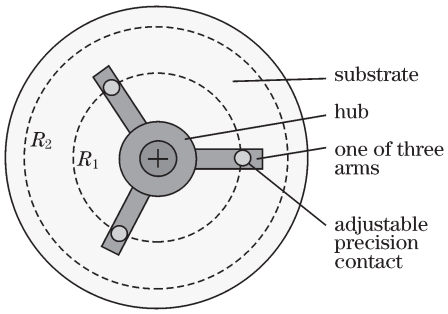

Fig. 4. Top down view sketch of a three-point contact hub.

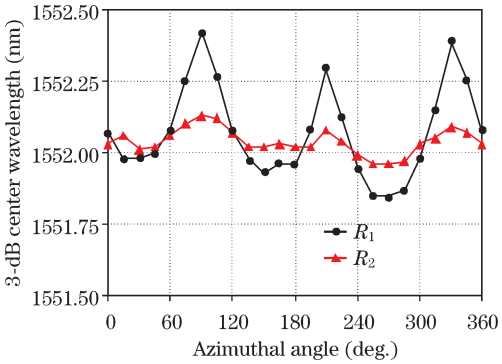

Fig. 5. Measured center wavelength of 100-GHz filter coated with three-point contact hub.

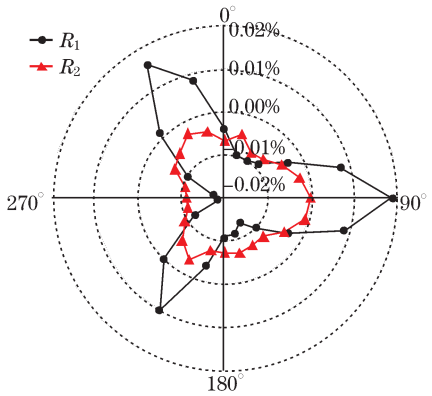

Fig. 6. Center wavelength placement variation from Fig. 5, expressed as a deviation percentage relative to the average center wavelength.

height to minimize variation. Using this setup height, we reduced height variations to less than 50 μm across the whole substrate coating surface.

Surprisingly, a sequence of coating runs did not yield the expected low runoff and repeatability. We measured azimuthal center wavelength distribution of a 100 GHz telecom filter at radii R_1 and R_2 (indicated as dashed lines in Fig. 4) in angular increments of 15°. Figure 5 shows center wavelength as a function of azimuth angle. Figure 6 shows the same information in a polar plot where center wavelength placement deviation is expressed as a percentage relative to average center wavelength.

Measured non-uniformity at radius R_1 is 0.6 nm, over 70% of the channel spacing from one 100 GHz filter to the next. Variation at radius R_2 is less, but still above 20% of channel spacing. Both center wavelength distributions have three lobes.

We hypothesized that this outcome was due to thermal effects. The hub was connected through the rotary drive shaft to the outside machine. Three arms of the hub rotated from the perspective of an observer outside the machine, but they were stationary with respect to the substrate. Three contact points created a temperature gradient across the substrate, locally reducing substrate temperature around the contact area, which affected the sticking coefficient or the refractive index, thus leading to variations in the center wavelength.

The example illustrates how subtle features in mechanical components can influence temperature distribution of a substrate, and how temperature distribution can limit the precision of a coating process. We were able to optimize the hub through further changes in geometry, size, and material selection.

A lost or moving anode is a well-known problem when reactively sputtering dielectrics, such as silica, alumina, and other metal oxides. In a standard direct current (DC) or pulsed DC sputtering process, the target acts as cathode, while the chamber wall acts as an anode. During deposition of non-conducting materials, the substrate and chamber walls become coated. The coating of "natural anode" or ground could change the electrical return path to the power supply. This behavior is known as a "moving anode", and can lead in its worst case known into a "lost anode"[4]. The "moving anode" results in a change of sputter distribution between the coating runs and within a coating run[5]. However, a "lost anode" causes extensive arcing at the cathode and the ground. A powered anode is a conductive surface that does not get coated, and is connected to the positive side of power supply. Bottle brush[6] and ring anodes[7] are typical anode geometries that have been used. Both have the disadvantage of becoming coated with insulating material as time progress, resulting in a change of plasma conditions.

A novel anode was designed for the JDSU's Metamode^{TM} platform. A detailed description of this coating platform is published in Refs. [8,9]. Main attributes of the anode, as shown in Fig. 7, are the relatively large anode area of about 0.2 m^2, a gas inlet that allows the anode to operate at a higher pressure than the chamber, and the opening of the anode with an area of about 2000 mm^2. The design does not have grounded surfaces close to the active anode area inside the tube.

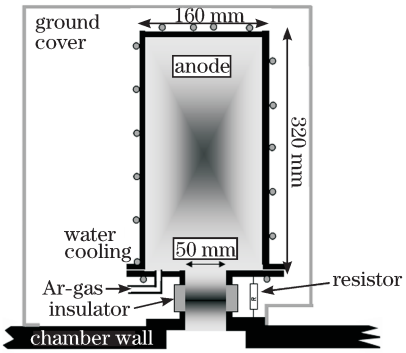

Fig. 7. Hollow anode for external mount.

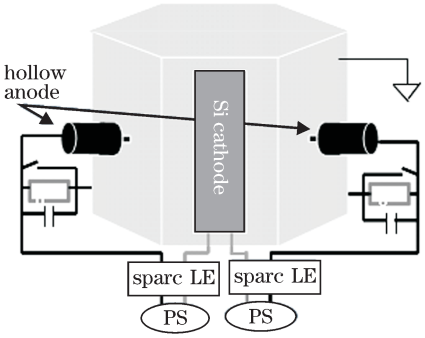

Fig. 8. Setup for hollow anode test in MetaMode^{TM} coating platform.

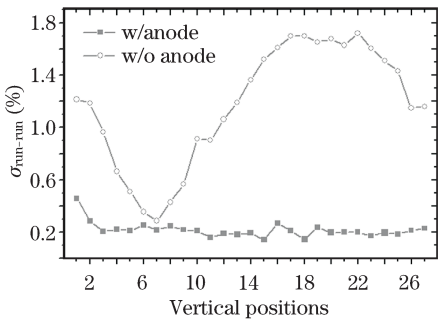

Fig. 9. Run-to-run variation of six consecutive coating runs with a hollow anode and without an anode, measured at 27 vertical positions that are spaced at ~ 45 mm.

A comprehensive description of the anode design follows the requirements determined in an extensive study [10].

Due to restricted space in the MetaMode^{TM} chamber, the anode was externally mounted to the chamber wall. To maintain a uniform vertical film thickness variation, two anodes were mounted symmetrically at the sides of the cathode, as illustrated in Fig. 8.

Two sets of six runs of SiO_2 single layers were coated at the same cathode power with a straight vertical cathode opening. One set was deposited with hollow anode configuration, and the other, without. We measured change in coating thickness at 27 vertical positions. Figure 9 shows the rate variation at different vertical drum positions. A drastic improvement in run-to-run variation of coating rates at different vertical positions was observed. Average variation improved from $\sigma = 1.0\%$ to $\sigma \approx 0.2\%$.

Many process improvements, including those described in this letter, were incorporated in JDSU's optical coating platform Ucp-1. The Ucp-1 is a high precision, high throughput magnetron sputtering platform designed for processing six 200-mm wafers. Load-lock and high deposition rates of about 1 nm/s for most of the coating materials enable very fast cycle times. For example, a 3-μm thick Ta_2O_5/SiO_2 multilayer filter can be manufactured in about an hour.

Process performance is shown in an example of a triple bandpass filter. These types of filters were developed for stereoscopic vision (three dimensions)[11]. They require accurate placement of passband and blocking regions. Figure 10 shows the performance of four consecutive coating runs. Variation between the four runs for a fully optimized machine under tight supervision was less than one nanometer at 572-nm edge.

Figure 11 shows the spectral performance of the same kind of filters within a coating run, measured at 30 positions (five measurements diagonally across each of the six wafers). Variation between all measurements is within 0.24% at 625-nm edge (Fig. 11(b)), which is equivalent to a standard deviation of $\sigma = 0.05\%$. On a routine basis for full batches, we can typically achieve a standard deviation of less than 0.3%.

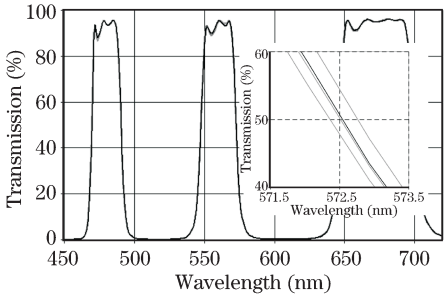

Fig. 10. Four consecutive coating runs of a triple bandpass filter. The insert shows the variation at 572-nm edge.

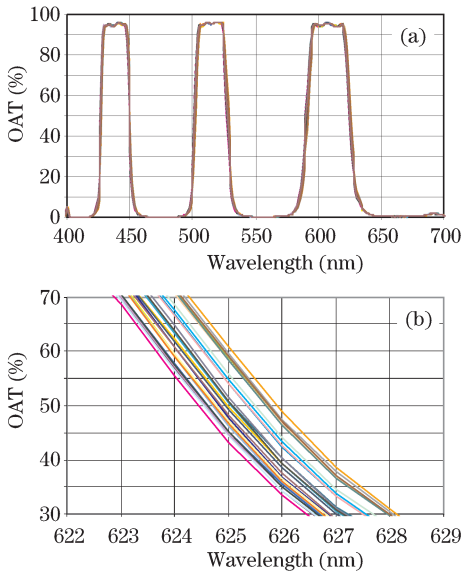

Fig. 11. Thirty measurements from a coating run: 6 wafers with 5 measurements across a 200-mm wafer, (a) overall performance; (b) spectral performance of 625-nm edge.

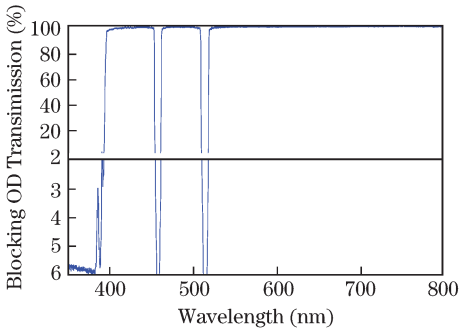

Fig. 12. Measurements of double narrow-band notch filter with OD6 blocking. Upper half of plot on linear scale, bottom half on logarithmic scale. (For text: 950 layers, 50-μm thick).

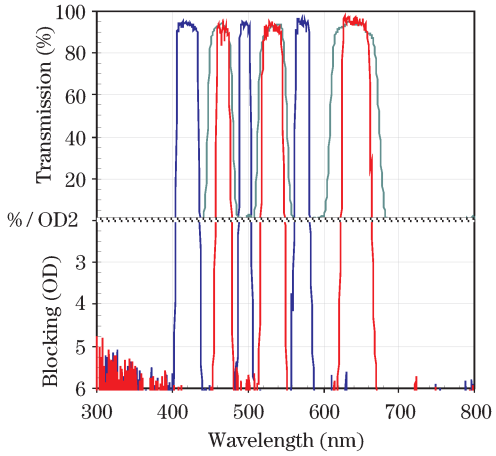

Fig. 13. Fluorescence filter set of triple bandpass filters for AMCA, FITC, and TexasRed fluorophores; Excitation (blue) and Emission (red) filters are measured at an incident angle of 0° and the polychroic beamsplitter (green) at 45°.

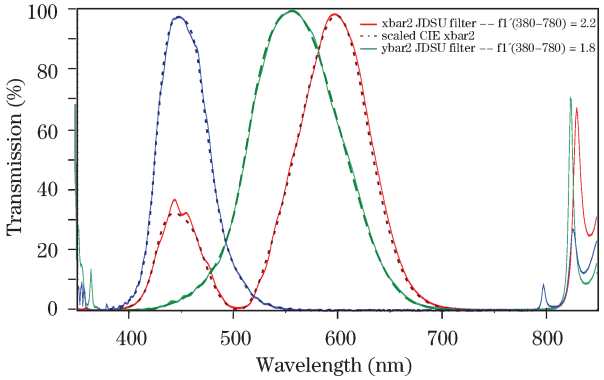

Fig. 14. Tristimulus filter set: solid lines indicate measurement and dashed ones represent CIE curves used as a target.

Ucp-1 coating platform enables the coating of very demanding thick coating designs. Figure 12 shows an example of a narrow double notch filter typically used in laser-based biomedical applications. The filter has over 950 layers and is over 50-μm thick. The main characteristics of this filter is the high transmission in the passband with extremely narrow notches with high blocking of optical density (OD) > 6 at the laser lines.

Another demanding filter set is presented in Fig. 13, which shows excitation, emission, and polychroic beamsplitter filters, enable to simultaneous excite and detect of fluorescence of three different fluorophores.

Due to improved process stability, filter designs that are not based on optical quarterwave stacks are possible to manufacture. An example of a tristimulus filter set built at CIE 1932 standard for a 2° observer is shown in Fig. 14. In the example, no blocking outside of 380–780 nm is added. Dashed lines in the graph represent targets, while solid lines represent measurements. These filters are used in colorimetry to measure and characterize color.

In conclusion, deterministic manufacturing of precision optical coatings requires a capable coating platform. In turn, the overall capability of a coating platform depends on the performance of its subsystems, which leads to stringent requirements on these subsystems. Here, we have presented examples illustrating these dependencies. In the first example, spectral placement tolerance was shown to drive the mechanical requirement of a rotary drive system. The second example showed how the run-to-run and within-run repeatability may require utilization of a powered anode to stabilize a DC sputtering process. Interactions between subsystems must also be accounted for. We described a circumstance in which a new method for holding a telecom substrate was developed to provide superior mechanical stability, and this worked well in accomplishing the intended purpose. However, the new method created a thermal gradient on the part that negatively affected the uniformity of the coating. Once a coating platform is optimized, it must be maintained in this condition. A problem with any of the subsystems can lead to drastic yield losses.

Impressive optical performance is attainable for complex filters when subsystems of a properly designed precision coating chamber work correctly. Here, coatings produced from the JDSU's Ucp-1 coating platform were provided as illustrations for triple bandpass, multiple-wavelength laser-line notch, and tristimulus filters.

We would like to thank our colleagues at JDSU who have contributed to this letter. Special thanks is also forwarded to Robert Sargent for his editorial assistance.

References

1. S. Sullivan, M. Tilsch, and F. Van Milligen, Photonics Spectra, November issue, Laurin Publishing (2005) p. 86.
2. R. Sargent, M. Tilsch, G. Ockenfuss, K. Hendrix, M. Grigonis, and A. Bergeron, in *Proceedings of SVC 51st Annual Technical Conference* O-1 (2008).
3. M. K. Tilsch, R. B. Sargent, and C. A. Hulse, *Wavelength Filters in Fibre Optics* H. Venghaus (ed.) (Springer Series in Optical Sciences, 2006) chap.7.
4. N. Boling, B. Wood, and P. Morand, in *Proceedings of SVC 38th Annual Technical Conference* 286 (1995).
5. P. Sieck, in *Proceedings of SVC 37th Annual Technical Conference* 233 (1994).
6. F. Gillery R. Criss, "Anode for magnetic sputtering apparatus" U.S. Patent 4,478,702 (1984).
7. F. Gillery and R. Criss, "Anode for magnetic sputtering of gradient films" U.S. Patent 4,744,880 (1988).
8. J. Seeser, P. LeFebvre, B. Hichwa, J. Lehan, S. Row-

lands, and T. Allen, in *Proceedings of SVC 35th Annual Technical Conference*, 229 (1992).

9. M. Scobey, R. Seddon, J. Seeser, R. Austin, P. LeFebvre, and B. Manley, "Magnetron sputtering apparatus and process" U.S. Patent 4,851,095 (1988).
10. G. J. Ockenfuss, M. K. Tilsch, and R. I. Seddon, *in Proceedings of 6th ICCG* 119 (2006).
11. H. Jorke, "Device for projecting a color image" U.S. Patent 6,698,890 (2004).